URL: http://dx.doi.org/10.1109/JSTQE.2010.2045476

Dynamic modeling of Terahertz Quantum Cascade Lasers

Yoann Petitjean, Fabien Destic, Jean-Claude Mollier *Member, IEEE,* and Carlo Sirtori, *Member, IEEE.*

***Abstract*—In this paper, the influence of the simplifications made in the four-equation-based set of rate equations describing the dynamic behavior of a Quantum Cascade Laser (QCL) is studied. Numerical simulations based on the set of four rate equations has been developed, enabling the theoretical study of the influence of different parameters on the direct modulation response of the laser. These equations have been then linearized in order to deduce a set of state system equations, which was written in a matrix formalism. Finally, an approximate second order transfer function has been derived with the linearized dependence of its times constant.**

***Index Terms*—Terahertz, Quantum Cascade Laser, modeling, dynamic behavior, bandwidth.**

I. Introduction

THIS paper aims at proposing a theoretical description of small signal modulation of Quantum Cascade Lasers (QCL). Their invention in 1994 by Faist, Capasso *et al.* [1] brought a powerful and compact solid source of far infrared radiation. Since then, their performances have continuously improved. Terahertz QCL working above liquid nitrogen temperature [2] [3], and even at room temperature by intracavity difference-frequency generation, have been reported [4]. Their spectral range is now extending from the mid-infrared down to 1.2 THz [5]. Due to the novel properties and unique interaction with many materials, the terahertz radiation has become a topic of active research for the past few years, and is still a going concern [6] [7]. Among the large possibilities of applications, free space short range communications have been studied [8] [9] because of the Wi-Fi capabilities of terahertz waves and QCL large supposed bandwidth modulation [10]. QCL-based local oscillators are also attractive for radioastronomy applications [11] thanks to their high spectral purity, adequate output power and good stability. Modeling the behavior of QCLs is therefore an important step toward the prediction of performances of such semi-conductor sources. Microscopic modelings have proved to be relevant in predicting and analyzing quantum device carrier dynamics and have largely participate to their design improvement [12] [13].

However, hereinbefore mentioned applications need a more global consideration of the optoelectronic system, and the establishment of a small signal equivalent circuit appears to be useful with this end in view. That is the final purpose of the theory presented in this paper. Indeed, theoretical study of electro-optical behavior, associated with the electrical ports S-parameters of a QCL should create a link between experimental measurements and intrinsic parameters values of the laser diode, and a better prediction of embedded device behavior. This method has proved to be apposite for many kinds of semiconductor lasers used in such applications. Macroscopic theoretical modeling of the QCL dynamic are easily usable: the set of rate equations governing the number of photons in the cavity and of electrons on the different possible states, along with their different lifetimes are sufficient. However, the microscopic theory is still needed to get a good description of the physical phenomena without introducing phenomenological parameters.

Considering the full rate equations system [14], a numerical simulation is firstly establish. It leads to modulation bandwidth up to a few dozens of gigahertz. Then, an analytical calculation is made to propose a transfer function that is simplified next, in order to study its dependence as a function of various parameters like lifetimes and number of periods.

January 30, 2010

A. Simplified QCL model

The simplified rate equations are based on a three-level classical scheme which leads to a 3 equations-system (2 for electrons on the two levels involved in the laser transition and 1 for photons). For a QCL of N_p periods, these equations are written as follows (Eq.(1) to (3)) [15] :

$$\frac{\partial N_3}{\partial t} = \eta \frac{I}{q} - \frac{N_3}{\tau_3} - G\left(N_3 - N_2\right) P \tag{1}$$

$$\frac{\partial N_2}{\partial t} = \frac{N_3}{\tau_{32}} - \frac{N_2}{\tau_2} + G\left(N_3 - N_2\right) P \tag{2}$$

$$\frac{\partial P}{\partial t} = N_p G\left(N_3 - N_2\right) P - \frac{P}{\tau_p} + \beta \frac{N_3}{\tau_{sp}} \tag{3}$$

where N_i is the number of electrons in the i^{th} level, P the number of photons, G the optical gain, τ_{32} the non-radiative scattering time, τ_i the electron lifetime in level i, and τ_p the photon lifetime. τ_{sp} is the spontaneous emission lifetime.

B. Benefits and inaccuracies of this model

These rate equations well describe the static behavior of quantum cascade lasers, as they lead to the same result than the full system as illustrated in fig.(1). The much more simple calculation needed for this model allows quite simple analytical results. Moreover, as other macroscopic theories

Y. Petitjean, F. Destic and J.C. Mollier are with the Institut Supérieur de l'Aéronautique et de l'Espace, 10 Av Edouard Belin, 31055 Toulouse Cedex, France.

J.C. Mollier is also with the French Aerospace Lab ONERA, 2 Av Edouard Belin, 31055 Toulouse Cedex, France.

C. Sirtori is with the University Paris 7, Matériaux et Phnomènes Quantiques, 10 rue A. Domont et L. Duquet, 75205 Paris Cedex 13, France.

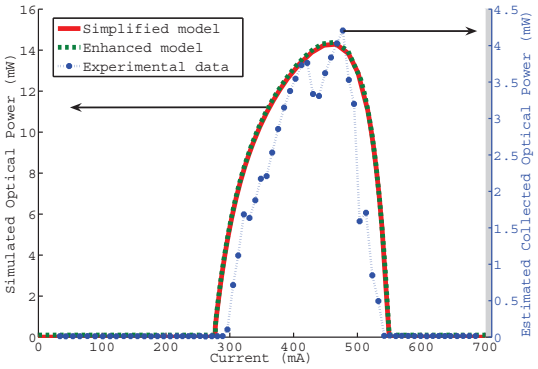

Fig. 1. Optical power versus current of a 30-periods QCL (dotted line : experimental data, solid line : simplified model and dashed line : enhanced model) [16]

that allow to deduce a small signal equivalent circuit, helpful for optoelectronic applications like direct intensity modulation communications, this modeling is very valuable.

However, this simplified modeling leads to a root-squared-law increase of the bandwidth with the number of periods. It is not a quite intuitive result. Indeed, the extraction time of the electrons to pass through the different periods is not taken into account. We can spontaneously think that this extraction time could decrease the small signal bandwidth of the QCL. That will be discussed further. Because of this simplification, small signal equivalent circuits deduced from this set of equations might lead to inaccuracies.

II. Full Rate Equations

The previous set of rate equations is actually deduced from a more complex one. In order to take into account the extraction time of the electrons to pass from the fundamental level of the i^{th} level to the excited one of the $i+1^{th}$ level, one more equation has to be reintegrated. The rate equations are consequently based on a three-level scheme with 4 equations (one for each of the three levels of the electrons and one for the photons) [14]. This so called full rate equation system is given by Eq.(4) to Eq.(7) :

$$\frac{\partial N_3^{(j)}}{\partial t} = \eta \frac{{I_{in}}^{(j)}}{q} - \frac{N_3^{(j)}}{\tau_3} - G^{(j)}\left(N_3^{(j)} - N_2^{(j)}\right) P \quad (4)$$

$$\frac{\partial N_2^{(j)}}{\partial t} = \frac{N_3^{(j)}}{\tau_{32}} - \frac{N_2^{(j)}}{\tau_2} + G^{(j)}\left(N_3^{(j)} - N_2^{(j)}\right) P \quad (5)$$

$$\frac{\partial N_1^{(j)}}{\partial t} = \frac{N_3^{(j)}}{\tau_{31}} - \frac{N_2^{(j)}}{\tau_{21}} - \frac{{I_{out}}^{(j)}}{q} \quad (6)$$

$$\frac{\partial P}{\partial t} = \sum_{j=1}^{N_p} G^{(j)}\left(N_3^{(j)} - N_2^{(j)}\right) P + n_{sp}\frac{N_3^{(j)} - N_2^{(j)}}{\tau_{sp}} - \frac{P}{\tau_p} \quad (7)$$

where N_i is the number of electrons in the i^{th} level, P the number of photons in the cavity, $G^{(j)}$ the optical gain of the j^{th} period, τ_i the electron lifetime in level i, and τ_p the photon lifetime. τ_{31}, τ_{32}, τ_{21} are the non radiative scattering times that are due to LO-phonon emission between the corresponding levels. n_{sp} is the spontaneous emission coefficient and τ_{sp} the radiative spontaneous relaxation time. $I_{in}^{(j)}$ and $I_{out}^{(j)}$ are respectively the input and output currents of the j^{th} period. For the first period, $I_{in}^{(1)}$ comes down to the input current of the QCL.

Moreover, in order to describe the cascade scheme of the QCL, since the input current of the j^{th} period is the output current of the $(j-1)^{th}$ period, these currents can be linked to a number of electrons extracted from the lower level of the $(j-1)^{th}$ period and injected on the upper level of the j^{th} period. Then, the output current of the j^{th} period is the rate of electrons leaving the level (1) given by Eq.(8) and the input current of the j^{th} period is the rate of electrons arriving on the level (3) from the level (1) of the previous period, given by Eq.(8).

$$\frac{{I_{out}}^{(j)}}{q} = \frac{N_1^{(j)}}{\tau_{out}} \quad (8)$$

$$\frac{{I_{in}}^{(j)}}{q} = \frac{N_1^{(j-1)}}{\tau_{out}} \quad (9)$$

III. Analytical Resolution

A. Hypotheses

The analytical resolution of the full rate equation is quite difficult for the time being. Consequently, one has to assume some simplifying hypotheses. First of all, the gain is supposed constant in the different periods. However, it could be an interesting job to focus on the spatial non-uniformity of the gain to describe furthermore the reality of the static and dynamic behavior. Secondly, the spontaneous emission term in the last equation is neglected as compared with the stimulated one. It is a well-known and quite correct assumption as soon as the laser is biased well above threshold. Last assumption, the η coefficient standing for the non-perfect injection of the electrons on the excited level will be supposed equal to 1. The value of this parameter has mainly an impact on the static behavior.

B. Linearized equations

From the rate equations above, a small perturbation method will be used to linearize them. Thus, the number of photons $P(t)$ will be the sum of the steady-state value P_0 and a small variation $p(t)$ around P_0. In the same way, the different numbers of electrons $N_i^{(j)}(t)$ in each level will be the sum of a steady-state term ${N_{i0}}^{(j)}$ and a perturbation one $n_i^{(j)}(t)$.

$$P(t) = P_0 + p(t) \quad with \quad p(t) \ll P_0 \quad (10)$$

$$N_i^{(j)}(t) = {N_{i0}}^{(j)} + n_i^{(j)}(t) \quad with \quad n_i^{(j)}(t) \ll {N_{i0}}^{(j)} \quad (11)$$

This method, associated with the previous hypotheses leads to a linearized set of four rate equations, given by Eq.(12) to (15) (the time dependence has been voluntarily omitted for clarity)

$$\frac{\partial n_3^{(j)}}{\partial t} = \frac{n_1^{(j-1)}}{\tau_{out}} - \frac{{n_3}^{(j)}}{\tau_3} - G\,(n_3^{(j)} - n_2^{(j)})\,P_0 - G\,\Delta N_0\,p \tag{12}$$

$$\frac{\partial n_2^{(j)}}{\partial t} = \frac{n_3^{(j)}}{\tau_{32}} - \frac{n_2^{(j)}}{\tau_2} + G\,(n_3^{(j)} - n_2^{(j)})\,P_0 + G\,\Delta N_0\,p \tag{13}$$

$$\frac{\partial n_1^{(j)}}{\partial t} = \frac{n_3^{(j)}}{\tau_{31}} - \frac{n_2^{(j)}}{\tau_{21}} - \frac{n_1^{(j)}}{\tau_{out}} \tag{14}$$

$$\frac{\partial p}{\partial t} = G\,P_0 \sum_{j=1}^{N_p}(n_3^{(j)} - n_2^{(j)}) + \left(G\,N_p\,\Delta N_0 - \frac{1}{\tau_p}\right)p \tag{15}$$

where $\Delta N_0 = {N_{30}}^{(j)} - {N_{20}}^{(j)}$ is a constant for the different period j and it is actually the case in the simulations.

Now, using Laplace formalism (s will be the Laplace variable and $X(s)$ the Laplace transform of $x(t)$), Eq.(16) to Eq.(19) are obtained :

$$\left(s + \frac{1}{\tau_3} + G\,P_0\right) N_3^{(j)}(s) = \frac{N_1^{(j-1)}(s)}{\tau_{out}} + G\,P_0\,N_2^{(j)}(s) - G\,\Delta N_0\,P(s) \tag{16}$$

$$\left(s + \frac{1}{\tau_2}\right) N_2^{(j)}(s) = \frac{N_3^{(j)}(s)}{\tau_{32}} + G\,P_0\,N_3^{(j)}(s) + G\,\Delta N_0\,P(s) \tag{17}$$

$$\left(s + \frac{1}{\tau_1}\right) N_1^{(j)}(s) = \frac{N_3^{(j)}(s)}{\tau_{31}} + \frac{N_2^{(j)}(s)}{\tau_{21}} \tag{18}$$

$$\left(s + \frac{1}{\tau_p} - G\,N_p\,\Delta N_0\right) P(s) = -G\,P_0 \sum_{j=1}^{N_p}\left(N_3^{(j)}(s) - N_2^{(j)}(s)\right) \tag{19}$$

C. Full QCL Matrix

The previous set of equations can be considered as a recurrent state system. Let us describe it thanks to a matrix formalism (Eq.(20)).

$$\left[\mathbb{A}\right]\cdot\left[\mathbb{N}^{(j)}\right] = \left[\mathbb{E}\right]\cdot\left[\mathbb{N}^{(j-1)}\right] + \left[\sigma\right]\cdot P(s) \tag{20}$$

Where $[\mathbb{A}]$ is the 3×3 state matrix of one period, $[\mathbb{E}]$ is also a 3×3 matrix that could be called the extraction matrix as it is a null matrix if the extraction time of the electrons is not taken into account, and $[\sigma]$ a 3×1 column matrix standing for the presence of photons in the electronic rate equations. These matrices are written as follows (Eq.(21) to Eq.(24)).

$$\left[\mathbb{N}^{(j)}\right] = \begin{bmatrix} N_3^{(j)}(s) \\ N_2^{(j)}(s) \\ N_1^{(j)}(s) \end{bmatrix} \tag{21}$$

$$\left[\mathbb{A}\right] = k\begin{bmatrix} s+\frac{1}{\tau_3}+G\,P_0 & -G\,P_0 & 0 \\ -\frac{1}{\tau_{32}}-G\,P_0 & s+\frac{1}{\tau_2}+G\,P_0 & 0 \\ -\frac{1}{\tau_{31}} & -\frac{1}{\tau_{32}} & s+\frac{1}{\tau_{out}} \end{bmatrix} = \begin{bmatrix} \alpha_{11} & \alpha_{12} & 0 \\ \alpha_{21} & \alpha_{22} & 0 \\ \alpha_{31} & \alpha_{32} & \alpha_{33} \end{bmatrix} \tag{22}$$

$$\left[\mathbb{E}\right] = \begin{bmatrix} 0 & 0 & -\frac{k}{\tau_{out}} \\ 0 & 0 & 0 \\ 0 & 0 & 0 \end{bmatrix} \tag{23}$$

$$\left[\sigma\right] = \begin{bmatrix} -\frac{\Delta N_0}{P_0} \\ \frac{\Delta N_0}{P_0} \\ 0 \end{bmatrix} = \begin{bmatrix} -\sigma \\ \sigma \\ 0 \end{bmatrix} \tag{24}$$

where $k = \frac{1}{G\,P_0} \approx 8.2\times 10^{-14}$ is a scale factor avoiding overflow during numerical computation.

This recurrent state system, associated with Eq. (19), can be described by a more complex state system allowing us to link the optical power $P_{opt}(s)$ to I(s). Indeed,

$$[\Omega]\cdot\begin{bmatrix} [\mathbb{N}^{(1)}] \\ [\mathbb{N}^{(2)}] \\ \vdots \\ [\mathbb{N}^{(j)}] \\ \vdots \\ [\mathbb{N}^{(N_p)}] \\ P(s) \end{bmatrix} = \begin{bmatrix} \frac{I(s)}{q\,G\,P_0} \\ 0 \\ \vdots \\ \\ \vdots \\ \vdots \\ 0 \\ 0 \end{bmatrix} \tag{25}$$

with :

$$[\Omega] = \begin{bmatrix} [\mathbb{A}] & [0] & \dots & & & [0] & [\sigma] \\ [\mathbb{E}] & [\mathbb{A}] & [0] & \dots & & : & [\sigma] \\ [0] & [\mathbb{E}] & [\mathbb{A}] & [0] & \dots & : & [\sigma] \\ : & \ddots & \ddots & \ddots & \ddots & : & : \\ : & & \ddots & \ddots & \ddots & [0] & : \\ [0] & \dots & \dots & [0] & [\mathbb{E}] & [\mathbb{A}] & [\sigma] \\ [\gamma] & \dots & & & \dots & [\gamma] & \delta \end{bmatrix} \quad (26)$$

$$[\gamma] = \begin{bmatrix} 1 & -1 & 0 \end{bmatrix} \quad (27)$$

$$\delta = k \left(s + N_p \, G \, \Delta N_0 + \frac{1}{\tau_p} \right) \quad (28)$$

$$P_{opt}(s) = \alpha_m \frac{c}{n_g} \, h \, \nu \, P(s) \quad (29)$$

n_g and α_m are respectively the mode-group index and the mirror losses.

D. Analytic Transfer Function Calculation

In order to calculate the transfer function of the QCL, the $(3\,N_p + 1)$ - by - $(3\,N_p + 1)$ $[\Omega]$ matrix has to be inverted using the well known method :

$$[\Omega]^{-1} = \frac{1}{det\,([\Omega])} \, {}^t Com\,([\Omega]) \quad (30)$$

In fact, only the $\{(3\,N_p + 1)\,; 1\}$ term of $[\Omega]^{-1}$, linking S(p) to I(p), is interesting. So, we just have to calculate the $\{1; (3\,N_p + 1)\}$ term of the co-matrix $Com\,([\Omega])$, which corresponds to the $\{1; (3\,N_p + 1)\}^{th}$ order minor determinant of $[\Omega]$ calculated by suppressing the 1^{st} line and the $(3\,N_p + 1)^{th}$ column (last one) of $[\Omega]$.

Then, the small signal electro-optical transfer function $H(s)$ is given by Eq.(31) :

$$H(s) = \frac{P_{opt}(s)}{I(s)} = \alpha_m \frac{c}{n_g} \frac{h\,\nu}{q} \, k \, \frac{(-1)^{(3N_p+2)} \, Cof_{1,Np}}{det\,([\Omega])} \quad (31)$$

with

$$det\,([\Omega]) = (-1)^{(3N_p+1)} \sigma \left(\sum_{k=0}^{N_p-1} (-d)^k \left(Cof_{1,N_p-k} + Cof_{2,N_p-k} \right) \right) + \delta \, d^{N_p} \quad (32)$$

in which $Cof_{i,k}$ is the minor determinant (co-factor) of a k-periods-QCL $[\Omega]$ matrix with the i^{th} line and last column suppressed. A recurrent relation on these determinants leads to the following general equations (Eq.(33) and Eq.(34)).

$$Cof_{1,k} = -Cof_{1,1} \sum_{i=0}^{k-1} \left(a_1^{k-i-1} \, d^i \right) \quad (33)$$

$$Cof_{2,k} = (-1)^{3N_p} \, a_2 \, Cof_{1,k-1} + Cof_{2,1} \, d^{k-1} \quad (34)$$

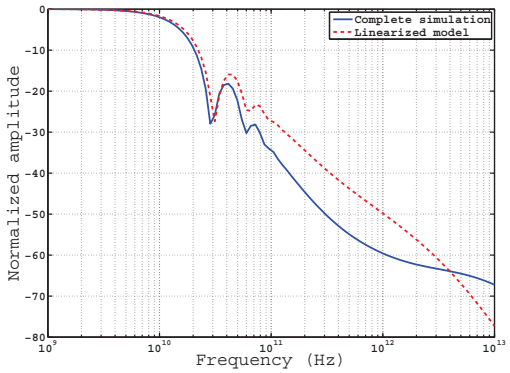

Fig. 2. Comparison between full numerical simulation and linearized state system of a 30-periods QCL at 450mA bias point.

with

$$a_1 = -\frac{k\,\sigma}{\tau_{out}} \left(\alpha_{21} \, \alpha_{32} - \alpha_{22} \, \alpha_{31} \right) \quad (35)$$

$$a_2 = -\frac{k\,\sigma}{\tau_{out}} \left(\alpha_{11} \, \alpha_{32} - \alpha_{12} \, \alpha_{31} \right) \quad (36)$$

$$d = det\,([\mathbb{A}]) \quad (37)$$

$$Cof_{1,1} = \sigma \, \alpha_{33} \left(\alpha_{21} + \alpha_{22} \right) \quad (38)$$

$$Cof_{2,1} = \sigma \, \alpha_{33} \left(\alpha_{11} + \alpha_{12} \right) \quad (39)$$

The higher degree Laplace terms 's' of this transfer function is $Cof_{1,1} \, d^{N_p - 1}$ for the numerator and $\delta \, d^{N_p}$ for the denominator. They respectively correspond to an s^{3N_p-1} term over an s^{3N_p+1}. Indeed, the higher degree term of $d = det\,([\mathbb{A}])$ is s^3, the higher one of δ is s, and the higher one of $Cof_{1,1}$ is s^2. Therefore, the calculation leads to a globally second-order transfer function.

IV. Simulations

A. Transfer Function Characteristics

From the study of the linearized bode diagram given in fig(2), we propose an approximate 2^{nd} order transfer function written as Eq.(40).

$$H(s) \approx H_0 \frac{1 + \tau_n \, s}{(1 + \tau_d \, s) \left(1 + \frac{2\,\xi}{\omega_0} \, s + \frac{s^2}{\omega_0^2} \right)} \quad (40)$$

with :

$$H_0 = \eta_i \frac{\alpha_m}{\alpha} \frac{h\,\nu}{q} \, N_p \approx 37 \; mW/A \quad (41)$$

where η_i is the internal quantum efficiency given by Eq.(42)

$$\eta_i = \frac{\tau_3 \left(1 - \frac{\tau_2}{\tau_{32}} \right)}{\tau_2 + \tau_3 \left(1 - \frac{\tau_2}{\tau_{32}} \right)} \quad (42)$$

Involved parameters values are given in table I.

TABLE I
DEVICE PARAMETERS USED IN NUMERICAL SIMULATIONS (UNLESS STATED OTHERWISE) (FROM [14], [15], [17], [18])

Parameter	Value
Lasing frequency ν (wavelength λ)	2.9 THz (103 μm)
Number of periods N_p	30
Confinement factor Γ	0.27
Cavity width w	80 μm
Cavity length L	3 mm
Facet reflectivity R	0.29
Mode-group index n_g	3.3
Cavity losses α_i	24cm^{-1}
Differential gain g	5×10^{-8} cm
Gain $G = g\,\Gamma\,\frac{c}{n_g\,L\,w}$	5.3×10^{4} s^{-1}
Equilibrium population inversion ΔN_0	10^5
Equilibrium photon number P_0 @$I_0 = 450mA$	2.3×10^{8}
τ_{out}	0.5 ps
τ_2	0.3 ps
τ_3	1.1 ps
τ_{31}	2.4 ps
τ_{32}	2 ps
τ_p	3.7 ps
τ_{sp}	7 ns

B. Evolution with various parameters

We can compute the dependence of τ_d, τ_n, ω_0 as a function of the number of periods N_p, the extraction time of the electrons τ_{out}, the lifetimes τ_2 and τ_{32}, and the number of photons in the cavity at equilibrium P_0.

Plots in fig.(3) to fig.(5) are the results of the simulations of the state system for several values of each parameter. In each case, only one parameter may vary, all others remaining constant and equal to the value given in table I.

Fig.(3) shows a very linear dependence of the inverse of the bandwidth, defined by a 3dB-decrease of the Bode response magnitude, as a function of N_p, τ_2, and τ_{out}. A linear fit of each plot leads to Eq.(43). The bandwidth is consequently linearly dependent on the inverse of the number of periods, which is a quite new result and implies a compromise between the optical power and the bandwidth. The variation of the bandwidth versus the inverse of the extraction time τ_{out} is understandable as the time taken by electrons to go from one period to the next should have an impact on the bandwidth. Linear dependence of the inverse of the bandwidth with respect to τ_2 is on the contrary a known result [15]. Other simulations have been made to study the dependence of the bandwidth on the photon lifetime τ_p with the result of a non-dependence, when τ_p varies in a range of a decade. This could be explained by the order of magnitude between the photon lifetime and the actual inverse of simulated bandwidth, the latter being indeed more driven by the carriers dynamic in the structure than the photon lifetime itself.

$$\omega_0 \approx \frac{1}{0.34\times10^{-12}\,N_p \;+\; 11.5\,\tau_{out} \;+\; 15\,\tau_2 \;-\; 7.8\times10^{-12}} \tag{43}$$

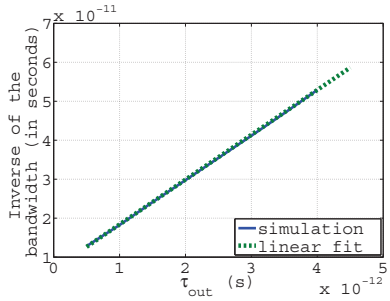

(a) Inverse of the bandwidth as a function of the extraction time τ_{out}

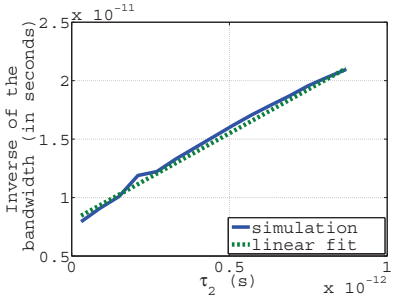

(b) Inverse of the bandwidth as a function of τ_2

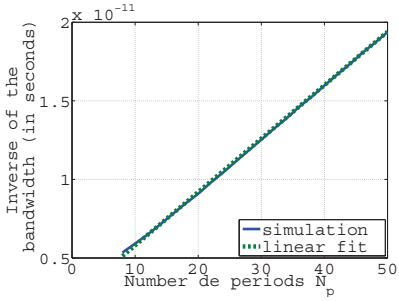

(c) Inverse of the bandwidth as a function of the number of periods N_p

Fig. 3. Variations of the inverse of the bandwidth with (a) τ_{out}, (b) τ_2 and (c) N_p. One can note the very linear dependence of the inverse of the bandwidth with these parameters.

The variations of τ_d with N_p and τ_d^{-1} with P_0 are quite linear. The step-like shape of the simulated curve in Fig.(4(b)) is only due to the precision of the numerical simulation. Eq.(44) can be considered to be a good approximation of τ_d variations against P_0 and N_p.

$$\tau_d \approx 1.65\times10^{-17}\,N_p \;+\; \frac{1}{2\,G\,P_0 \;+\; \frac{1}{\tau_2} \;-\; \frac{1}{\tau_{32}}} \tag{44}$$

The variations of τ_n with τ_{out}, τ_2 and N_p are much more complicated. Indeed, there is no simple relationship between these parameters as shown in fig.(5). Nevertheless, the variations of τ_n can be roughly linearized around the nominal values of τ_{out}, τ_2 and N_p given in table I to obtain Eq.(45). For a more accurate model, a higher degree polynomial form to fit τ_n variations can be used.

$$\tau_n \approx 4.3\times10^{-15}\,N_p \;+\; 2.5\,\tau_{out} \;+\; 3\,\tau_2 \;-\; 1.4\times10^{-12}$$

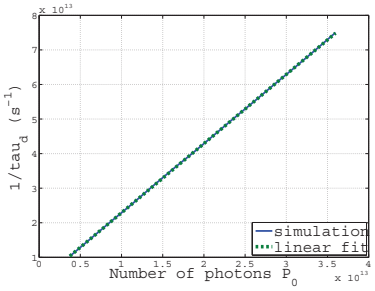

(a) Inverse of τ_d as a function of P_0

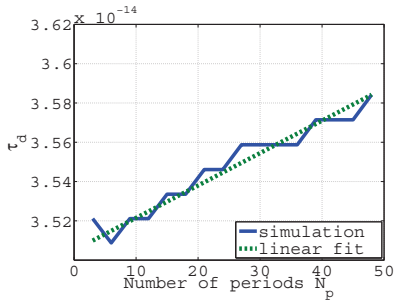

(b) τ_d as a function of the number of periods N_p

Fig. 4. Variations of τ_d with (a) P_0 and (b) N_p.

(45)

The two time constants τ_n and τ_d have not a major impact on the bandwidth as their numerical value is at least one order of magnitude less than the inverse of the bandwidth. However, they partially shape the Bode response magnitude in the high frequency domain (above the 3dB bandwidth) and their value is still important to extract parameter values like scattering times for instance.

V. Prospectives

In order to experimentally establish the bandwidth of QCLs, a test bench has been developed. It consists in a home-made electro-optical probe station, based on a TK1813 QMC Instruments Ltd. cryostat. A Cascade Microtech microwave probe and special feedthrough allow applying both the bias and modulation current up to 40 GHz. This probe is driven by a three-axis micrometer stage. Two others three-axis micrometer stages drive two optical 1,55 μm focalizers. Indeed, as there is not currently fast enough THz detector available, an up-conversion toward telecoms wavelength has been planned [19] [20]. Because of the second order non-linear susceptibility χ_2 of GaAs, the whole THz spectra with microwave modulation sidebands is shifted on both sides of the telecom wavelength line. Modulation frequencies as high as 13 GHz [21] and more recently, 24GHz [22] have been achieved with this technique. This test bench will allow us to have access to the Bode diagram magnitude of a QCL to validate our modeling. Based on this theory, work is in progress to propose small signal equivalent circuit of QCL, helpful for direct modulation applications. The different elements of the circuit are then link to intrinsic parameters and optimization of the QCL in accordance with the application is possible. It is also an

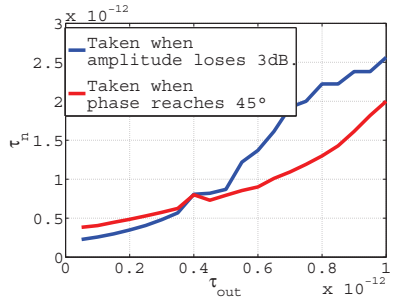

(a) τ_n as a function of the extraction time τ_{out}

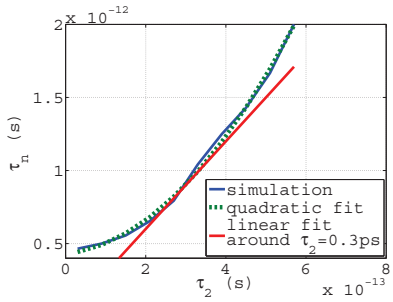

(b) τ_n as a function of τ_2

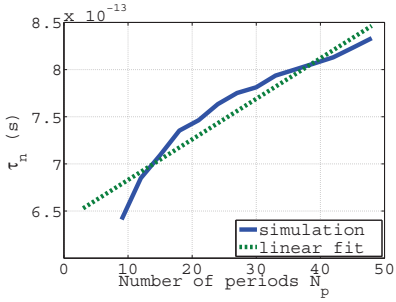

(c) τ_n as a function of the number of periods N_p

Fig. 5. Plots of the variations of τ_n with (a) τ_{out}, (b) τ_2 and (c) N_p. The dependence of τ_n with these various parameters is obvious, but not simple like a linear one.

efficient method to get access to the intrinsic parameters of the laser chip under test and to evaluate the device features, in the same way as the technique used for more conventional lasers like VCSELs [23].

VI. Conclusion

A simplified transfer function, taking account of QCL cascade scheme architecture has been presented. The time constant variations of this transfer function have been pointed out and lead to a dependence of the direct modulation bandwidth with the number of periods and the electron extraction time. Numerical functions have been proposed, that could be useful as a way of prediction of dynamic QCL performances. Further work and experiments are in progress to experimentally prove these dependences.

Acknowledgment

The authors would like to thank Stefano Barbieri, from University Paris 7 Diderot, laboratoire Matériaux et Phénomènes Quantiques, for the supply in QCLs.

REFERENCES

[1] J. Faist, F. Capasso, D. L. Sivco, C. Sirtori, A. L. Hutchinson, and A. Y. Cho, "Quantum cascade laser," *Science*, vol. 264, April 1994.

[2] G. Scalari, L. Ajili, J. Faist, H. Beere, E. Linfield, D. Ritchie, and G. Davies, "Far-infrared bound-to-continuum quantum-cascade lasers operating up to 90 k," *Applied Physic Letters*, vol. 82, May 2003.

[3] S. Kumar, Q. Hu, and J. L. Reno, "186 k operation of terahertz quantum-cascade lasers based on a diagonal design," *Applied Physic Letters*, vol. 94, April 2009.

[4] M. A. Belkin, F. Capasso, F. Xie, A. Belyanin, M. Fischer, A. Wittmann, and J. Faist, "Room temperature terahertz quantum cascade laser source based on intracavity difference-frequency generation," *Applied Physic Letters*, vol. 92, May 2008.

[5] C. Walther, M. Fischer, G. Scalari, R. Terazzi, N. Hoyler, and J. Faist, "Quantum cascade lasers operating from 1.2 to 1.6 thz," *Applied Physic Letters*, vol. 91, September 2007.

[6] P. H. Siegel, "Terahertz technology," *IEEE Transaction on Microwave Theory and Technique*, vol. 50, March 2002.

[7] D. Saeedkia and S. Safavi-Naeini, "Terahertz photonics: Optoelectronic techniques for generation and detection of terahertz waves," *IEEE Journal of lightwave technology*, vol. 26, August 2008.

[8] F. Capasso, R. Paiella, R. Martini, R. Colombelli, C. Gmachl, T. L. Myers, M. S. Taubman, R. M.Williams, C. G. Bethea, K. Unterrainer, H. Y. Hwang, D. L. Sivco, A. Y. Cho, A. M. Sergent, H. C. Liu, and E. A. Whittaker, "Quantum cascade lasers: Ultrahigh-speed operation, optical wireless communication, narrow linewidth, and far-infrared emission," *IEEE Journal of Quantum Electronics*, vol. 38, June 2002.

[9] R. Piesiewicz, M. Islam, M. Koch, and T. Kurner, "Towards Short-Range Terahertz Communication Systems: Basic Considerations," in *ICECom*, 2005.

[10] N. Mustapha, L. Pesquera, C. Y. L. Cheung, and K. A. Shore, "Terahertz bandwidth prediction for amplitude modulation response of unipolar intersubband semiconductor lasers," *IEEE Photonics Technology Letters*, vol. 11, May 2005.

[11] J. R. Gao, J. N. Hovenier, Z. Q. Yang, J. J. A. Baselmans, A. Baryshev, M. Hajenius, T. M. Klapwijk, A. J. L. Adam, and T. O. Klaassen, "Terahertz heterodyne receiver based on a quantum cascade laser and a superconducting bolometer," *Applied Physic Letters*, vol. 86, June 2005.

[12] R. C. Iotti and F. Rossi, "Microscopic modelling of opto-electronic quantum devices: A predictive simulation tool," *Journal of Computational Electronics*, vol. 2, December 2004.

[13] ——, "Microscopic modelling of semiconductor-based quantum devices: a predictive simulation strategy," *Physica status solidi B*, vol. 238, July 2003.

[14] F. Rana and R. J. Ram, "Current noise and photon noise in quantum cascade lasers," *Physical Review B*, vol. 65, March 2002.

[15] M. K. Haldar, "A simplified analysis of direct intensity modulation of quantum cascade laser," *IEEE Journal of Quantum Electronics*, vol. 41, November 2005.

[16] Y. Petitjean, F. Destic, and J.-C. Mollier, "Bandwidth simulation and measurement of Terahertz Quantum Cascade Laser," in *IRMMW-THz*, 2009.

[17] J. Faist, L. Ajili, G. Scalari, M. Giovannini, M. Beck, M. Rochat, H. E. Beere, A. G. Davies, E. H. Linfield, and D. A. Ritchie, "Terahertz quantum cascade laser," *The Royal Society*, December 2003.

[18] C. Sirtori, "Quantum cascade laser : fundamentals and performances," in *EDP sciences*, 2002.

[19] S. S. Dhillon, C. Sirtori, S. Barbieri, A. de Rossi, M. Calligaro, H. E. Beere, and D. A. Ritchie, "Thz sideband generation at telecom wavelengths in a gaas-based quantum cascade laser," *Applied Physic Letters*, vol. 87, March 2005.

[20] S. S. Dhillon, C. Sirtori, J. Alton, S. Barbieri, A. de Rossi, H. E. Beere, and D. A. Ritchie, "Terahertz transfer onto a telecom optical carrier," *Nature Photonics*, vol. 1, July 2007.

[21] S. Barbieri, W. Maineult, S. S. Dhillon, C. Sirtori, J. Alton, N. Breuil, H. E. Beere, and D. A. Ritchie, "13 ghz direct modulation of terahertz quantum cascade lasers," *Applied Physic Letters*, vol. 91, August 2007.

[22] W. Maineult, L. Ding, P. Gellie, P. Filloux, C. Sirtori, S. Barbieri, T. Akalin, J.-F. Lampin, I. Sagnes, H. E. Beere, and D. A. Ritchie, "Microwave modulation of terahertz quantum cascade laser : a transmission-line approach," *Applied Physic Letters*, vol. 96, January 2010.

[23] A. Bacou, A. Hayat, V. Iakovlev, A. Syrbu, A. Rissons, J.-C. Mollier, and E. Kapon, "Electrical modeling of long-wavelength vcsels for intrinsic parameters extraction," *IEEE Journal of Quantum Electronics*, vol. 46, March 2010.

Yoann Petitjean (S06) was born in Epinal, France, in 1982. He received the M.S. degree (with honors) in microwaves and opto-electronics from the Institut Supérieur de l'Aéronautique et de l'Espace (ISAE), Université de Toulouse, France, in 2007. He also received the french examination called "Agrégation" in electric engineering in 2006 (very high level, national competitive examination for the recruitment of the best teachers in France, giving the equivalent of a university title). His research interests include QCL-based terahertz active imaging and terahertz quantum cascade laser simulation and characterization, which is the PhD subject he is preparing.

Fabien Destic worked as an engineer for a French military agency in the field of laser granulometry, from 1985 to 1991. Since 1991, he is at ISAE where he specialized in fiber optic telecoms and telecom lasers characterization. After a Master in Microwave and Optoelectronic in 2005 from Toulouse University, he is now a PhD student on QCL-based THz active imaging.

Jean-Claude Mollier (M97) received the Doctorate degree from the University of Franche-Comté, Besançon, France, in 1982. He then joined the Laboratoire de Physique et Metrologie des Oscillateurs, where he was involved with stable RF oscillators. In 1984, he joined the Research Institute in Optical and Microwave Communications (XLIM), Limoges, France, where he became Manager of a research group in the field of broadband and low-noise microwave amplification. Since 1991, he has been involved with microwavephotonic interactions with SUPAERO-ONERA, Toulouse, France. He is currently Head of the Department of Electronics-Optronics-Signals (DEOS), Institut Supérieur de l'Aéronautique et de l'Espace (ISAE), Toulouse, France. His research interests include optical generation of microwave signals, modeling and characterization of semiconductor lasers (VCSELs and quantum cascade lasers) for application in optical fiber links and terahertz active imaging. Dr. Mollier is a member of the IEEE Lasers and Electro-Optics Society (IEEE LEOS) and the French Optical Society (SFO), where he founded the Optics and Microwaves Club in 1995.

Carlo Sirtori received his PhD in physics at the University of Milan in 1990. The same year he joined Bell Labs where he started his research carrier on quantum devices. During the 7 years spent at Bell Labs, he made important contributions such as the invention and the development of the "Quantum Cascade Laser". In 1997, Carlo Sirtori joined the "Laboratoire Central de Recherche of Thomson-CSF (currently Thales Research & Technology, TRT) near Paris. In 2000 he was appointed head of the "Semiconductor Laser Group" and responsible of the clean room at TRT for the development of semiconductor lasers in the near- and mid-infrared. During he developed the first quantum cascade laser based on GaAs/AlGaAs and the concept of plasmonic waveguides for semiconductor lasers. In 2002, he was appointed Professor at the University Paris Diderot - Paris 7, where he pursues his research on unipolar quantum devices. Carlo Sirtori is the author of more than 170 articles in peer reviewed journals, he has given 60 invited talks at international conferences. He has received several prestigious awards such as the Fresnel Prize (European Physical Society) and various prizes in the USA, such as the "quantum devices award". In 2010 he has been awarded of an ERC-advanced-grant for his pioneering research on quantum devices. He also member of the Institut Universitaire de France.